(Figure 2). Although the resulting interdimer Cu···Cu separation is actually smaller (7.2571 (7) Å) than the intradimer Cu···Cu distance (8.0020 (6) Å), the difference of effectiveness between the two exchange pathways (intermolecular vs intramolecular) is surprising. Furthermore, the interdimer bridge is from an axial position at one copper atom to another axial position at the second copper and it is well-known that, for copper ions assuming square-based configurations, the spin density along these axial direction is very low. As noted elsewhere,[50] more data are needed to rationalize the ability of the extended bridging network to support significant magnetic data.

Acknowledgment. We thank Dr. Mari for his contribution to the magnetic measurements.

Registry No. I, 137918-27-5; II, 137918-29-7; III, 86959-37-7; $[TmenCuOH]_2(ClO_4)_2$, 14266-63-8.

Supplementary Material Available: Tables SI–SIV, listing hydrogen atomic positional and thermal parameters, final anisotropic thermal parameters, bond lengths and angles, and least-squares planes equations for I (5 pages); a table of calculated and observed structure factor amplitudes for I (15 pages). Ordering information is given on any current masthead page.

(50) Colacio, E.; Costes, J.-P.; Kivekas, R.; Laurent, J.-P.; Ruiz, J.; Sundberg, M. *Inorg. Chem.* **1991**, *30*, 1475 and references therein.

Contribution from the School of Chemical Sciences and Beckman Institute, University of Illinois, Urbana-Champaign, Urbana, Illinois 61801

A Molecular Mechanics Model of Ligand Effects. 2. Binding of Phosphines to $Cr(CO)_5$

Kevin J. Lee and Theodore L. Brown*

Received May 1, 1991

Molecular mechanics methods have been employed to compute the energy-minimized structures of a series of 19 trialkylphosphines and their complexes with $Cr(CO)_5$. The comprehensive computational package BIOGRAF was employed, using the MMP2 force field. The computed structure of $Cr(CO)_5PMe_3$ is in good agreement with the structural parameters determined by X-ray diffraction. The ligand–metal complex steric interaction is often manifested in a tilting of the ligand with respect to the Cr–P bond, especially in the most unsymmetrical ligands. The Cr–P distance increases with increasing value of ligand cone angle. For the largest ligands, $P(t\text{-}Bu)_2(i\text{-}Pr)$ and $P(t\text{-}Bu)_3$, the Cr–P distance is about 0.39 Å longer than expected from extrapolation of the data for smaller ligands, indicative that excessive steric repulsions prevent normal metal–ligand bond formation. Excepting the two longest distances, the variation in Cr–P distance with cone angle is roughly linear, with a dependence on cone angle more than twice as great as for the phosphite complexes, reported earlier. The total energy varies monotonically with increasing ligand cone angle. However, the only component of the total energy change that varies in a regular way is the bond energy term. As ligand steric requirement increases, increasing van der Waals repulsive interactions between ligand and complex are offset by variations in corresponding attractive terms. Thus, there is not a regular increase in the total van der Waals energy with increasing cone angle. The structure of $Cr(CO)_5PMe_3$ was determined by conventional crystallographic techniques with Mo Kα X-rays. At −75 °C, the crystals belong to monoclinic space group $P2_1/c$ with a = 6.946 (2) Å, b = 11.622 (3) Å, c = 14.935 (3) Å, β = 103.16 (2)°, V = 1174 (1) Å^3, and Z = 4.

In the first paper of this series, we described a molecular mechanics model for the interaction between phosphorus ligands and a metal center and its application to the interaction of a series of phosphites with $Cr(CO)_5$.[1] In this contribution, we describe the application of the model to interaction of a series of trialkylphosphines with $Cr(CO)_5$. Throughout the series, there is a substantial variation in steric requirement, as a result of branching at either α- or β-carbon positions.

There are no published structural data available for a trialkylphosphine complex of $Cr(CO)_5$. As a means of further testing the computational results, we have obtained the crystal structure of $Cr(CO)_5PMe_3$.

Methods

Computations were carried out using BIOGRAF, a comprehensive package of molecular modeling tools developed and marketed by Molecular Simulations, Inc., of Sunnyvale, CA. The force field model employed is MMP2.[2] The components of the energy terms in the calculations are described in detail in a previous paper.[1] Table I lists added or modified parameters, where these differ from the standard MMP2 set or those listed in the previous paper. The major difference from the set employed with the phosphites consists in a longer equilibrium Cr–P bond of 2.35 Å, as compared with 2.30 Å assumed for the phosphites. The methods employed for locating minimum-energy structures have been described.[1]

It has been assumed in the computations that complex formation causes an increase in the equilibrium C–P–C bond angle in the ligand, from 93° characteristic of the free ligand to 100° characteristic of the complexed ligand. This assumption is consistent with molecular orbital calculations[3] as well as with the observed structural data. It results in essentially the same computed variations in energies as when a constant equilibrium value of 93° is assumed.

Experimental Section

All manipulations were carried out under an argon atmosphere using standard Schlenk techniques. Reagent grade CH_2Cl_2 (Fischer) was distilled from P_2O_5 under N_2. The following chemicals were obtained from commercial sources and used as received: Me_3PAgI (Aldrich), $AgNO_3$ (Mallincrodt), and reagent grade hexane (Aldrich). $Et_4N[Cr(CO)_5Cl]$ was prepared as described in the literature.[4] Solution infrared spectra were recorded on a Perkin-Elmer 1710 FT-IR spectrometer using a 0.5 mm path length cell with KCl windows.

$Cr(CO)_5PMe_3$ was prepared by a modification of a published procedure.[5] $Et_4N[Cr(CO)_5Cl]$ (0.736 g, 2.06 mmol) and $AgNO_3$ (0.560 g, 3.30 mmol) were dissolved in 100 mL of CH_2Cl_2. The solution turned dark orange, and a white precipitate formed. After 10 min of stirring, a solution containing Me_3PAgI (0.643 g, 2.07 mmol) dissolved in 35 mL of CH_2Cl_2 was added via cannula. Additional white precipitate formed. After 10–15 min, the solvent was removed in vacuo, leaving a white residue which gradually turned gray. The gray residue was extracted with 100 mL of hexane, and the volume was reduced in vacuo to about 4 mL. Storage of this solution at −20 °C produced large colorless needles of $Cr(CO)_5PMe_3$. (ν_{CO}(hexane) 2063 w, 1951 m, 1939 vs cm^{-1}; lit.[5] 2064 w, 1952 m, 1941 vs cm^{-1}).

X-ray Crystal Structure Determination of $Cr(CO)_5PMe_3$

A colorless, transparent, prismatic crystal with well-developed faces was mounted to a thin glass fiber. Diffraction data were collected at −75 °C on an Enraf-Nonius CAD4 automated κ-axis diffractometer employing Mo Kα (λ = 0.71071 Å) radiation. The intensity data were

(1) Caffery, M. L.; Brown, T. L. *Inorg. Chem.* **1991**, *30*, 3907–3914.
(2) (a) Burkert, U.; Allinger, N. L. *Molecular Mechanics*; ACS Monograph 177; American Chemical Society: Washington, DC, 1982. (b) Sprague, J. T.; Tai, J. C.; Yuh, Y.; Allinger, N. L. *J. Comput. Chem.* **1987**, *8*, 581.
(3) Magnuson, E. *Aust. J. Chem.* **1985**, *38*, 23.
(4) Wovkulich, M. J.; Atwood, J. D. *Organometallics* **1982**, *1*, 1316.
(5) Connor, J. A.; Jones, E. M.; McEwen, G. K. *J. Organomet. Chem.* **1972**, *43*, 357.

0020-1669/92/1331-0289$03.00/0

Table I. Added Parameters for MMP2 Force Field Calculations

A. Bond Stretching Parameters

bond type	k_s,[a] mdyn/Å	r_0, Å
Cr–P	2.000	2.350
P–C(sp^3)	2.910	1.810
Cr–C(sp) radial	2.100	1.880
Cr–C(sp) axial	2.100	1.850
C(sp)–O(sp) radial	17.040	1.120
C(sp)–O(sp) axial	17.040	1.150
O(sp)–LP[b]	4.601	0.600

B. Bond Angle Bending Parameters

bond angle type	k_b, mdyn Å/rad^2	θ, deg	1st angle-stretch force const, mdyn/rad	2nd angle-stretch force const, mdyn/rad
P–C(sp^3)–H	0.360	111.0	0.090	0.000
P–C(sp^3)–C(sp^3)	0.480	111.5	0.120	0.120
C(sp^3)–P–C(sp^3)	0.576	100.0	0.200	0.200
Cr–P–C(sp^3)	0.209	112.0	0.000	0.000

C. Dihedral Angle Torsions[c]

torsional type	periodicity	$K_{\phi,n}$, kcal/mol	phase factor
P–C(sp^3)–C(sp^3)–H	3	0.330	−1
P–C(sp^3)–C(sp^3)–C(sp^3)	3	0.400	−1
H–P–C(sp^3)–H	3	0.428	−1
H–P–C(sp^3)–C(sp^3)	1	−0.530	−1
H–P–C(sp^3)–C(sp^3)	2	−0.400	1
H–P–C(sp^3)–C(sp^3)	3	0.600	−1
C(sp^3)–P–C(sp^3)–H	1	0.050	−1
C(sp^3)–P–C(sp^3)–H	3	0.420	−1
C(sp^3)–P–C(sp^3)–C(sp^3)	1	0.200	−1
C(sp^3)–P–C(sp^3)–C(sp^3)	3	0.500	−1

[a] Multiply by 143.88 to convert from mdyn/Å to (kcal/mol)/Å^2. [b] LP = lone pair. [c] The force constants for all dihedral angles involving the chromium atom were set to zero.

Table II. Crystallographic Data for $Cr(CO)_5PMe_3$

chem formula	$C_8H_9O_5CrP$	temp, °C	−75
fw	268.13	size, mm	0.6 × 0.8 × 0.8
space group	$P2_1/c$	ρ_{calcd}, g cm^{-3}	1.517
a, Å	6.946 (2)	μ, cm^{-1}	10.81
b, Å	11.622 (3)	transm coeff	0.528, 0.451
c, Å	14.935 (3)	$R(F_o)$,[a] %	3.1
β, deg	103.16 (2)	$R_w(F_o)$,[b] %	4.1
V, Å^3	1174 (1)	Δ/σ	0.003
Z	4	Δ/ρ, e Å^{-3}	0.43

[a] $R = \sum||F_o| - |F_c||/\sum|F_o|$. [b] $R_w = (\sum w(|F_o| - |F_c|)^2/\sum w|F_o|^2)^{1/2}$; $w = 2.16/[(\sigma(F_o))^2 + (0.02F_o)^2]$.

corrected for Lorentz, polarization, anomalous dispersion, and absorption effects. No problems were encountered, and no change in the appearance of the crystal occurred during data collection. The details of the structure determination and the crystallographic data for $Cr(CO)_5PMe_3$ are given in Table II.

The structure was solved by Patterson methods (SHELXS-86). The correct position for the chromium atom was deduced from a vector map, and partial structure expansion gave positions for the phosphorus atom and CO groups. Subsequent least-squares-difference Fourier calculations gave positions for the remaining atoms. The hydrogen atoms were included as fixed contributors in idealized positions. During the final cycle of refinement, thermal coefficients were varied for non-hydrogen atoms and independent isotropic thermal coefficients were refined for hydrogen atoms. The final difference Fourier map had no significant features.

Results

Calculated values of important bond distances and angles in the free ligands and $Cr(CO)_5$ complexes are available as supplementary material. Table III lists the calculated total molecular mechanics energies, E_T, of ligands and complexes, and the values for the bond stretch (E_b), bond bend (E_θ), dihedral angle torsion (E_ϕ), and van der Waals (E_{vdW}) energy components of the total energy. Table IV lists the molecular mechanics energy differences corresponding to complex formation; see eq 1, where E_{Cr-P}, E_P,

$$\Delta E = E_{Cr-P} - E_P - E_{Cr} \quad (1)$$

and E_{Cr} correspond to the total energy or one of the components of the total energy for $Cr(CO)_5PR_3$, PR_3, and $Cr(CO)_5$, respectively. The energy terms corresponding to the energy-minimized structure for $Cr(CO)_5$ are $E_T = E_{vdW} = -2.21$ kcal mol^{-1} and $E_b = E_\phi = 0$.

Table V lists the important bond distances and angles in $Cr(CO)_5PMe_3$, as obtained from the X-ray structure determination. Figure 1 shows a view of the molecular structure.

Discussion

For convenience in drawing comparisons, Table VI lists the values obtained for several bond distances and angles for $Cr(CO)_5PMe_3$ from the X-ray structure determination and from the molecular mechanics calculation. For this simple substance, with zero overall charge and with no alkyl chains of extended length, the condensed-phase structure should not differ significantly from that for the isolated molecule. Thus, the excellent agreement between observed and computed structures suggests that the set of parameters chosen for the molecular mechanics calculations are appropriate. It is noteworthy that there is a slight tilting of the PMe_3 ligand with respect to the Cr–P bond axis. Although intermolecular interactions may contribute, tilting arises mainly because of the dissimilar orientations of the the three methyl groups with respect to the CO groups in the $Cr(CO)_4$ plane. One methyl group (C_6 in Figure 1) is oriented near the center of an angle between cis CO groups; the other two methyl groups are more nearly eclipsed with respect to Cr–CO bond axes. A similar tilting effect is seen in the crystal structures of $Cr(CO)_5PR_2R'$

Table III. Calculated Molecular Mechanics Energies (kcal mol^{-1}) of the Unbound Phosphines and Corresponding $Cr(CO)_5PR_3$ Complexes in Their Minimum-Energy Configurations

	free phosphine					$Cr(CO)_5PR_3$ complexes				
ligand	E_T	E_b	E_θ	E_ϕ	E_{vdW}	E_T	E_b	E_θ	E_ϕ	E_{vdW}
PMe_3	0.32	0.00	0.46	0.91	−1.05	−6.29	0.02	0.53	0.71	−7.55
PMe_2Et	1.47	0.05	0.69	1.06	−0.33	−5.57	0.09	0.98	0.87	−7.51
PEt_2Me	2.64	0.11	1.00	1.18	0.34	−4.61	0.22	1.49	1.02	−7.34
PEt_3	3.92	0.17	1.32	1.27	1.17	−3.00	0.27	2.52	1.25	−7.04
P(*n*-Bu)$_3$	7.53	0.61	1.96	1.32	3.63	−0.65	0.71	3.07	1.30	−5.73
PMe_2(*i*-Pr)	2.81	0.23	0.95	1.19	0.45	−3.81	0.35	1.67	1.07	−6.90
PMe_2(*t*-Bu)	5.55	0.58	2.54	1.28	1.15	−0.87	0.92	2.68	1.21	−5.68
PEt_2(*i*-Pr)	6.16	0.30	2.95	1.45	1.46	−0.63	0.62	3.35	1.56	−6.16
P(*i*-Bu)$_3$	8.04	0.86	2.73	1.34	3.11	6.75	1.40	5.84	4.93	−5.42
P(*i*-Pr)$_2$Me	6.40	0.42	2.83	1.51	1.64	0.01	0.91	3.18	1.50	−5.58
PEt_2(*t*-Bu)	9.21	0.74	3.19	2.31	2.97	3.77	1.65	4.23	2.49	−4.60
P(*i*-Pr)$_2$Et	8.77	0.49	3.78	2.03	2.47	3.61	1.38	4.74	2.06	−4.57
P(*i*-Pr)$_3$	12.16	0.61	5.51	3.25	2.80	9.21	2.11	6.42	3.49	−2.81
P(*t*-Bu)$_2$Me	14.38	1.22	6.92	2.63	3.62	12.27	3.41	7.31	2.69	−1.14
P(*t*-Bu)$_2$Et	17.28	1.39	8.01	3.01	4.87	16.01	4.38	8.53	3.23	−0.13
P(*i*-Pr)$_2$(*t*-Bu)	16.64	1.10	7.85	3.27	4.42	15.10	3.54	8.27	4.22	−0.93
PCy_3	26.20	1.34	6.31	9.65	8.90	25.13	2.97	7.37	12.07	2.72
P(*t*-Bu)$_2$(*i*-Pr)	21.93	1.38	11.80	3.85	4.90	24.39	8.72	11.68	3.80	0.18
P(*t*-Bu)$_3$	28.49	2.31	14.19	3.90	8.09	35.85	11.63	13.88	5.32	5.02

Table IV. Differences in the Computed Molecular Mechanics Energies (kcal mol^{-1}) upon Complex Formation (ΔE in Eq 1)

ligand	ΔE_T	ΔE_b	ΔE_θ	ΔE_ϕ	ΔE_{vdW}	θ, deg
PMe_3	−4.40	0.02	0.07	−0.20	−4.29	118
PMe_2Et	−4.83	0.04	0.29	−0.19	−4.97	123
PEt_2Me	−5.03	0.11	0.49	−0.16	−5.47	127
PEt_3	−4.72	0.10	1.20	−0.02	−6.00	132
$P(n\text{-}Bu)_3$	5.96	0.10	1.11	−0.02	−7.15	132
$PMe_2(i\text{-}Pr)$	−4.50	0.12	0.72	−0.12	−5.22	132
$PMe_2(t\text{-}Bu)$	−4.21	0.34	0.14	−0.07	−4.62	139
$PEt_2(i\text{-}Pr)$	−4.60	0.32	0.40	0.09	−5.44	141
$P(i\text{-}Bu)_3$	0.91	0.54	3.11	3.58	−6.32	143
$P(i\text{-}Pr)_2Me$	−4.18	0.49	0.35	−0.01	−5.01	146
$PEt_2(t\text{-}Bu)$	−3.23	0.91	1.04	0.18	−5.36	149
$P(i\text{-}Pr)_2Et$	−2.95	0.89	0.96	0.03	−4.83	151
$P(i\text{-}Pr)_3$	−0.75	1.50	0.91	0.24	−3.40	160
$P(t\text{-}Bu)_2Me$	0.09	2.19	0.39	0.06	−2.55	161
$P(t\text{-}Bu)_2Et$	0.94	2.99	0.52	0.22	−2.79	165
$P(i\text{-}Pr)_2(t\text{-}Bu)$	0.67	2.44	0.42	0.95	−3.14	167
PCy_3	1.14	1.63	1.06	2.42	−3.97	170
$P(t\text{-}Bu)_2(i\text{-}Pr)$	4.66	7.34	−0.12	−0.05	−2.51	175
$P(t\text{-}Bu)_3$	9.56	9.31	−0.31	1.42	−0.86	182

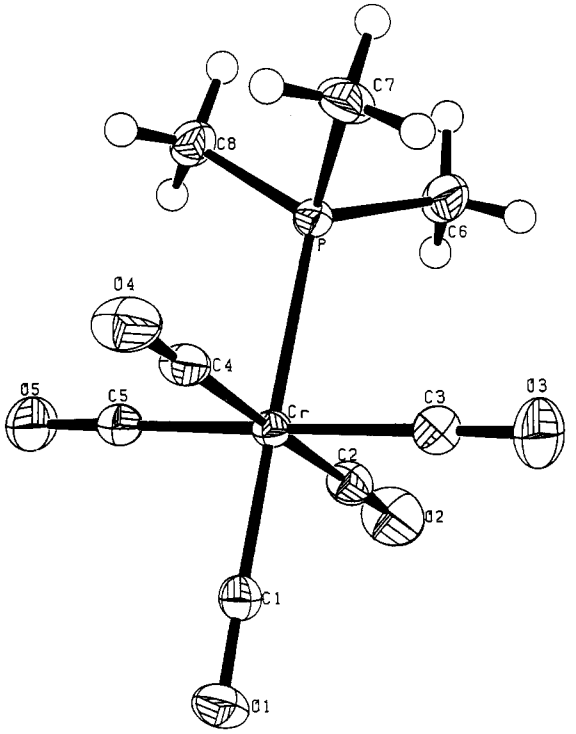

Figure 1. View of one molecule of $Cr(CO)_5PMe_3$ in the molecular structure, as determined by X-ray diffraction analysis. The thermal ellipsoids for non-hydrogen atoms are shown for the 35% level.

(R = R′ = CH_2CH_2CN,[6] Ph;[7] R = Me, R′ = SH[8]) as well as $W(CO)_5PMe_3$.[9]

Tilting of the ligand in this manner is increasingly evident in the molecular mechanics calculations as the ligand becomes less symmetric. Figure 2 shows the energy-minimized structure of $Cr(CO)_5P(t\text{-}Bu)_2Me$. In this case, the methyl group is forced into the space between cis Cr–CO bonds as the ligand tilts to relieve steric repulsions between the two *tert*-butyl groups and nearby CO groups. The result is that the Cr–P–C angle for the methyl group is only 105.6 °C, while those for the two *tert*-butyl groups are 116.9 and 118.6°.

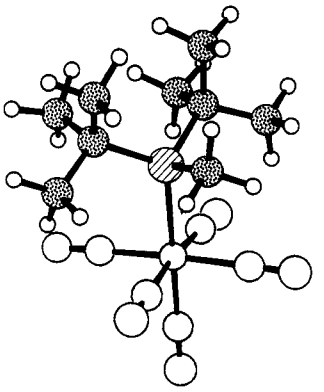

Figure 2. Energy-minimized structure for $Cr(CO)_5P(t\text{-}Bu)_2Me$.

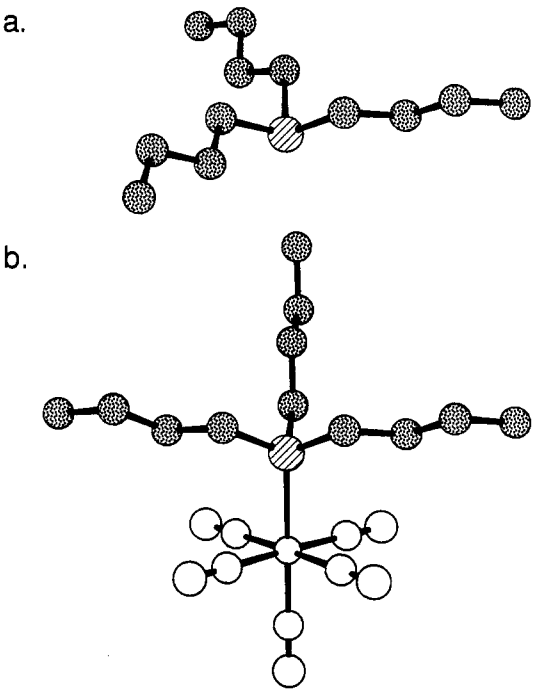

Figure 3. Energy-minimized structures for (a) $P(n\text{-}Bu_3)$ and (b) $Cr(CO)_5P(n\text{-}Bu)_3$.

Changes in ligand conformation and evidences of ligand distortion are also manifested in the computed structures. Figure 3 shows that the conformation of $P(n\text{-}Bu)_3$ changes significantly on complex formation. The free ligand has 3-fold axial symmetry. In the complex, two of the butyl groups are disposed differently from the third because they have a different relationship to the CO groups of the metal carbonyl fragment. Similarly, in free PCy_3 all three cyclohexyl rings are in the chair conformation, with the bonds to phosphorus in equatorial positions, as expected.[10] In the complex, however, one of the cyclohexyl rings is distorted to a "twist" conformation because of steric repulsions with the nearest metal carbonyl group.

Increasing steric repulsions between groups bound to the phosphorus as the group sizes increase are evidenced by increases in the P–C bond distances, from 1.85 Å for the smallest ligands to 1.88 Å for the largest. Similarly, the C–P–C angles in both the free ligands and in the complexes increase with increasing bulk of the alkyl group. Evidences for increasing steric repulsion between ligand and metal carbonyl complex are seen in a decrease in C_{ax}–Cr–C_{rad} angles and increasing Cr–P distance as the ligand size increases. These changes are due entirely to the effects of repulsive interactions on bond distances and angles as the system seeks a minimum energy configuration; the assumed "strain-free"

(6) Cotton, F. A.; Darensbourg, D. J.; Kolthammer, W. S. *Inorg. Chem.* **1981**, *20*, 4440.
(7) Plastas, H. J.; Stewart, J. M.; Grim, S. O. *Inorg. Chem.* **1973**, *12*, 265.
(8) Meier, v. W.-P.; Strahle, J.; Linder, E. *Z. Anorg. Allg. Chem.* **1976**, *427*, 154.
(9) Cotton, F. A.; Darensbourg, D. J.; Ilsley, W. H. *Inorg. Chem.* **1981**, *20*, 578.
(10) Carey, F. A.; Sundberg, R. J. *Advanced Organic Chemistry*, 2nd ed.; Plenum Press: New York, 1984; pp 111–123.

Table V. Bond Distances and Bond Angles from the X-ray Crystal Structure of $Cr(CO)_5PMe_3$

(a) Bond Distances (Å)

Cr–P	2.3664 (5)	O2–C2	1.137 (3)	O4–C4	1.136 (2)	P–C6	1.813 (2)
Cr–C1	1.850 (2)	Cr–C3	1.891 (2)	Cr–C5	1.897 (2)	P–C7	1.815 (2)
O1–C1	1.153 (2)	O3–C3	1.134 (2)	O5–C5	1.129 (2)	P–C8	1.814 (2)
Cr–C2	1.894 (2)	Cr–C4	1.888 (2)				

(b) Bond Angles (deg)

Cr–P–C6	115.98 (9)	Cr–P–C7	114.66 (7)	Cr–P–C8	116.82 (7)
C6–P–C7	102.6 (1)	C6–P–C8	102.89 (10)	C7–P–C8	101.85 (10)
P–Cr–C1	178.23 (6)	P–Cr–C2	90.68 (6)	P–Cr–C3	88.16 (6)
P–Cr–C4	88.04 (6)	P–Cr–C5	90.79 (6)	C1–Cr–C2	90.77 (8)
C1–Cr–C3	90.82 (8)	C1–Cr–C4	90.54 (8)	C1–Cr–C5	90.25 (8)
C2–Cr–C3	90.07 (8)	C2–Cr–C4	178.21 (8)	C2–Cr–C5	89.25 (8)
C3–Cr–C4	91.13 (8)	C3–Cr–C5	178.74 (8)	C4–Cr–C5	89.52 (9)
Cr–C1–O1	178.9 (2)	Cr–C2–O2	178.3 (2)	Cr–C3–O3	178.5 (2)
Cr–C4–O4	179.3 (2)	Cr–C5–O5	179.2 (2)		

Table VI. Comparison of the Values for Key Bond Distances (Å) and Angles (deg) from the X-ray Crystal Structure for $Cr(CO)_5PMe_3$ with the Values Computed Using MMP2

bond or angle	crystal structure	MMP2 minimum-energy structure
Cr–P	2.366	2.360
P–C6	1.813	1.811
P–C7	1.815	1.811
P–C8	1.814	1.810
Cr–C1	1.850	1.850
Cr–C2	1.894	1.879
Cr–C3	1.891	1.879
Cr–C4	1.888	1.880
Cr–C5	1.897	1.880
C6–P–C7	102.6	102.1
C6–P–C8	102.9	102.6
C7–P–C8	101.9	102.5
P–Cr–C2	90.68	90.53
P–Cr–C3	88.16	89.55
P–Cr–C4	88.04	90.40
P–Cr–C5	90.79	91.14
Cr–P–C6	116.0	115.7
Cr–P–C7	114.7	115.1
Cr–P–C8	116.8	116.9

values of the parameters are the same throughout the series.

There is a small but steady increase in Cr–P distance with increasing ligand cone angle, from 2.360 Å for $Cr(CO)_5PMe_3$ to 2.416 Å for PCy_3. For complexes of the two ligands of still larger steric requirement, $Cr(CO)_5P(t\text{-}Bu)_2(i\text{-}Pr)$ and $Cr(CO)_5(t\text{-}Bu)_3$, the equilibrium Cr–P distance is much larger, 2.73 and 2.74 Å, respectively. The large values of Cr–P distance indicate that the repulsive interactions between ligand and the metal complex are too large to permit formation of a normal Cr–P bond. The particular range of Cr–P distance at which the ligand–metal interaction is established in these cases is an artifact of the cubic form assumed for the stretching potential (eq 2), which is designed

$$E_b = (k_b/2)(r - r_0)^2[1 + d(r - r_0)] \qquad (2)$$

to take account of anharmonicity in the stretching vibration at large displacements from equilibrium. Typically, $d = -2$. To prevent dE_b/dr becoming negative, the sign of dE_b/dr is reversed in BIOGRAF for $r - r_0$ values larger than $-2/3d$. For $d = -2$, the inflection point occurs at $r - r_0 = 0.33$. The computed values of Cr–P distance for the $P(t\text{-}Bu)_3$ and $P(t\text{-}Bu)_2(i\text{-}Pr)$ complexes correspond to $r - r_0$ values of 0.38–0.39. The computed Cr–P distances for these two complexes are clearly not comparable with the values for the other ligands. The *significant* result is that the molecular mechanics model predicts that these two ligands will not form normal complexes with $Cr(CO)_5$.

Unfortunately, no crystal structure data are available in the literature for $Cr(CO)_5$ complexes with phosphines of large cone angle. The $Cr(CO)_5P(i\text{-}Pr)_3$ complex can be prepared in the same way as described for $Cr(CO)_5PMe_3$, but repeated attempts to obtain crystals suitable for X-ray analysis were unsuccessful. On the basis of crystal structure determinations, the W–P distances

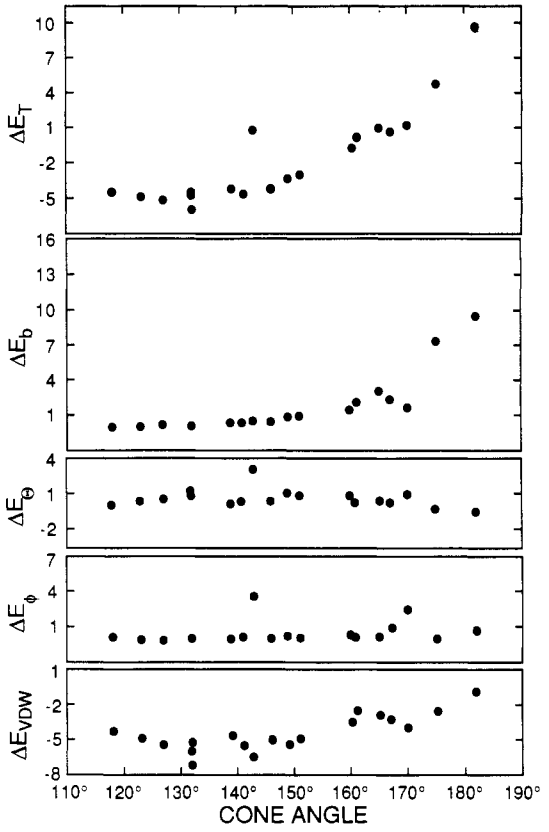

Figure 4. Total molecular mechanics energy change upon complex formation, ΔE_T, and the components of ΔE as a function of increasing cone angle of the ligand, for trialkylphosphine complexes of $Cr(CO)_5$.

in $W(CO)_5PMe_3$[6] and $W(CO)_5P(t\text{-}Bu)_3$[11] have been determined to be 2.516 (2) and 2.686 (4) Å, respectively. The large increase in bond length suggests that the W–P bond is substantially weakened in the $P(t\text{-}Bu)_3$ complex as compared with the PMe_3 derivative. The steric effect should be substantially larger for the Cr complexes because of the smaller metal covalent bond radius. We were unsuccessful in attempts to prepare $Cr(CO)_5P(t\text{-}Bu)_3$. A low-temperature matrix synthesis of a weakly bound adduct should be possible.

In Figure 4 are displayed the variations in the total energy change and components of the energy change for complex formation, as a function of the cone angle value for the ligand. Note that the energy scale is the same for each component. With the exception of the energy variation of $Cr(CO)_5P(i\text{-}Bu)_3$, the total energy change is more or less independent of cone angle at values below about 145° and then increases with cone angle at higher values. Rather strikingly, the principal component of this change

(11) Pickhardt, V. J.; Rosch, L.; Schumann, H. *Z. Anorg. Allg. Chem.* **1976**, *426*, 66.

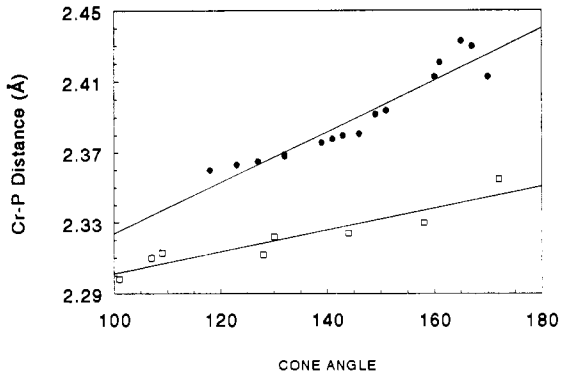

Figure 5. Variations in Cr–P distance with ligand cone angle for trialkylphosphine (●) and phosphite (□) complexes of $Cr(CO)_5$. The lines represent linear least-squares fits to the two data sets.

is the bond stretch component. No secular changes occur in ΔE_θ or ΔE_ϕ. The variation in ΔE_{vdW} is rather irregular, though there is an upward trend for ligands of large cone angle.

As pointed out previously,[1] the ΔE_{vdW} term contains contributions from both repulsive and attractive van der Waals terms. As the groups attached to the phosphorus grow more highly branched, their repulsive interactions with one another and with the CO groups of the $Cr(CO)_5$ fragment increase. At the same time, the longer range attractive interactions increase. There is therefore an irregular relationship with cone angle, because the two terms tend to cancel. It is noteworthy that ΔE_{vdW} is negative for all ligands in the series; in the molecular mechanics model, the sum of new attractive energy terms occasioned by complex formation is larger than the corresponding sum of new repulsive energy terms.

While the repulsive component of ΔE_{vdW} is related to the steric property of the ligand, the attractive term is not; it is an electronic property of the ligand, related to its polarizability. A conceptually analogous categorization of substituent effects has long been employed in the analysis of organic systems.[12] A more detailed discussion of this point is reserved for the following paper in this series.

The bending and torsional components of the energy change on complex formation are substantially different for $P(i\text{-}Bu)_3$ from those for the other ligands. The anomalous behavior, reflected in the value for ΔE_T, results from the fact that $P(i\text{-}Bu)_3$ is branched in the β position of the carbon chain. It is possible for the free ligand to adopt a conformation that does not result in internal repulsive interactions giving rise to bond bends and torsional distortions; note that the free-ligand energy terms are consonant with those of the other ligands (Table III). In the complex, however, the constraints imposed on the Cr–P–C–C dihedral angles by repulsive interactions with $Cr(CO)_5$ result in unavoidable internal repulsions. The recognition of such an energy term is not new; Brown and co-workers in their pioneering work on steric effects referred to the phenomenon as "backstrain".[13] The effect has not been widely recognized, however, as important in affecting the properties of ligands. This example points illustrates the importance of components of the total energy change on complex formation that, while they can be construed as steric in origin, are not adequately reflected in the cone angle. The anomalously large ΔE value is consistent with empirical evidence based on free energy correlations of kinetics data, which indicate that $P(i\text{-}Bu)_3$ possesses a larger cone angle than the assigned value.[14,15]

The phosphine complexes behave similarly to the phosphite complexes[1] in that the total energy change upon complex formation generally increases as a function of cone angle. However, in the

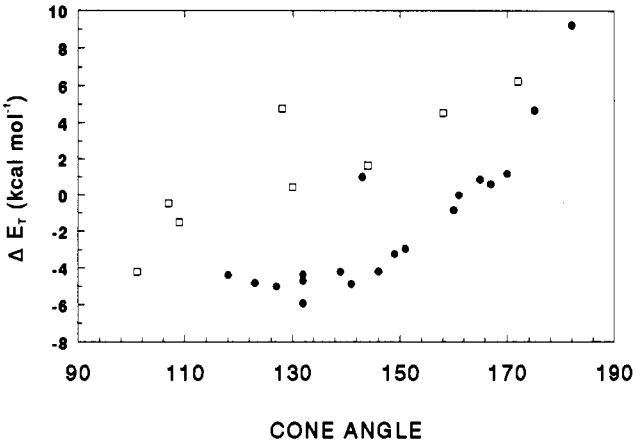

Figure 6. ΔE_T vs cone angle for trialkylphosphine (●) and phosphite (□) complexes of $Cr(CO)_5$.

phosphite series the major component of the energy change is bond bending, whereas in the phosphines it is bond stretching. Figure 5 shows the variation in Cr–P distance with ligand cone angle for the phosphites and phosphines, omitting the two phosphine complexes for which the Cr–P distance is very large. There is a roughly linear dependence on cone angle in each case. The dependence is clearly larger for the phosphines; the slope of the linear relationship is 1.4×10^{-3} Å/deg vs 6.2×10^{-4} Å/deg for the phosphites. In the phosphite series, the steric repulsions between the ligand and $Cr(CO)_5$ fragment are absorbed more readily in bond bending, including the "bending" of oxygen lone pairs. One way of putting it is that the phosphites are more flexible ligands than phosphines.

The question arises as to whether the constancy of ΔE_T with cone angle to about 140° and the monotonic increase with cone angle beyond this point should be described as a "steric threshold".[16,17] We believe that the computational result may correspond to experimentally observed behavior ascribed to steric thresholds. At the same time, interpretation of the experimental results in terms of the model presented here involves more than merely the onset of a repulsive interaction. The repulsive component alone increases steadily with increasing cone angle, even for small ligands.[18] However, for the smaller ligands, this increase may be offset by increasing dispersion force attractive interactions. As the ligand becomes still larger, as reflected in a cone angle value greater than about 140° in the case of the $Cr(CO)_5$ complexes, the increase in the van der Waals repulsive term becomes increasingly dominant, producing changes in other components of the molecular mechanics energy, with a net increase in ΔE_T.

In these terms, the steric threshold will not necessarily arise, in that it depends on the balancing of energy terms of opposite sign for a group of ligands. The relative importance of the repulsive and attractive van der Waals components varies from one class of ligand to another. Figure 6 shows ΔE_T vs cone angle for the phosphite and phosphine series. For the same value of cone angle, ΔE_T is substantially larger for the phosphites, and there is no sign of a steric threshold. Because the components of the total energy vary with cone angle in different manners for the phosphites and phosphines, there is no simple accounting for the difference predominantly in terms of one component of the energy change.

The major lessen to be drawn from these comparisons is that the molecular mechanics energetics of complex formation do not depend in a simple way on the particular dimension of ligand character that is reflected in the cone angle. As indicated above, the van der Waals attractive term plays a major role in deter-

(12) Taft, R. W.; Topsom, R. D. *Prog. Phys. Org. Chem.* **1987**, *16*, 1.
(13) (a) Brown, H. C.; Bartholomay, H., Jr.; Taylor, M. D. *J. Am. Chem. Soc.* **1944**, *66*, 435.
(14) (a) Hanckel, J. M.; Lee, K.-W.; Rushman, P.; Brown, T. L. *Inorg. Chem.* **1986**, *25*, 1852.
(15) Leising, R. A.; Ohman, J. S.; Takeuchi, K. J. *Inorg. Chem.* **1988**, *27*, 3804.
(16) (a) Golovin, M. N.; Rahman, Md. M.; Belmonte, J. E.; Giering, W. P. *Organometallics* **1985**, *4*, 1981. (b) Rahman, Md. M.; Liu, H. Y.; Prock, A.; Giering, W. P. *Organometallics* **1987**, *6*, 650.
(17) Brodie, N. M. J.; Chen, L.; Poë, A. J. *Int. J. Chem. Kinet.* **1988**, *20*, 467.
(18) Brown, T. L. *Inorg. Chem.*, submitted for publication.

mining the total energy change in the molecular mechanics model. This very significant contribution to the total energy of complex formation can be expected to appear as a component of the total energetics of complex formation measured experimentally. However, the attractive term is not part of what is traditionally referred to as the steric property of a ligand. For this reason, it is necessary to employ the results of the molecular mechanics calculations in a different way to extract a quantity that properly reflects the purely steric properties of the ligands. An approach to this goal is described in the following paper in this series.[18]

Acknowledgment. This research was supported by the National Science Foundation through Research Grant NSFCHE89-12273. K.J.L. gratefully acknowledges a University of Illinois Graduate Fellowship (1986-7) and a Department of Education Graduate Fellowship (1989-90). BIOGRAF was made available through an academic grant from Molecular Simulations, Inc. The Stardent Titan computer on which the calculations were carried out was obtained through a University Research Initiative award from the Defense Advanced Research Projects Agency. The crystal structure determination of $Cr(CO)_5PMe_3$ was carried out in the X-ray Diffraction Center of the School of Chemical Sciences by Scott Wilson.

Supplementary Material Available: Tables of crystallographic data, data collection and reduction parameters, information on solution and refinement, atomic positional parameters, and thermal parameters for $Cr(CO)_5PMe_3$, a table of selected bond distances and angles in the energy-minimized structures for the free phosphine ligands, tables of selected bond distances and angles in the energy-minimized structures for $Cr(CO)_5PR_3$ complexes, and figures showing unit cell views for $Cr(CO)_5PMe_3$ (12 pages), a listing of structure factor amplitudes for $Cr(CO)_5PMe_3$ (18 pages).

Contribution from the Departamento de Quimica Inorgânica, Universidad de Valencia, 46100 Burjassot, Valencia, Spain, and Dipartamento di Chimica, Universitâ di Firenze, 50144 Firenze, Italy

Anisotropic Exchange and Dimerization in the Ordered Bimetallic Chains $Co_2(EDTA)\cdot 6H_2O$ and $CoCu(EDTA)\cdot 6H_2O$. Single-Crystal EPR Investigation

Juan J. Borrâs-Almenar,[†] Eugenio Coronado,*[,†] Dante Gatteschi,*[,‡] and Claudia Zanchini[‡]

Received May 8, 1991

The bimetallic series $MM'(EDTA)\cdot 6H_2O$ ([MM'] = [MnCo], [MnNi], [MnCu], [CoCo], [CoNi], [CoCu], [NiNi]) comprises zigzag chains built up with alternated "hydrated" and "chelated" sites bridged by carboxylate groups: ...-$M(H_2O)_4O_2$---M'(EDTA)-$M(H_2O)_4O_2$---M'(EDTA)-.... The **g** tensors of cobalt(II) on both sublattices are determined from a single-crystal EPR study on Co-doped [ZnZn] samples. On the other hand, a single-crystal EPR study of the bimetallic chain [CoCu] is reported. The angular dependence of the resonance fields are simulated from a triplet spin state with a large zero-field splitting of modulus $|D| \approx 0.3$ cm^{-1}, which is almost parallel to the **g** tensor of cobalt. This result provides some evidence of the presence of cobalt-copper exchange-coupled pairs within the chain, constituting the first spectroscopic proof of dimerization in this chain; furthermore, it emphasizes the anisotropic nature of the exchange, which is in good agreement with the spin anisotropy of cobalt. The factors determining the dimerization of this and other cobalt-containing chains of the EDTA series are discussed.

Introduction

For the past few years much experimental and theoretical effort has been devoted to the properties of one-dimensional (1-D) ferrimagnets, in particular to their static thermodynamic properties (specific heat, magnetic susceptibility, magnetization, etc.).[1-4] In this context, the bimetallic compounds of the EDTA family formulated as $MM'(EDTA)\cdot 6H_2O$ (in short [MM']) provided a remarkable series of magnetic model systems for investigating a great diversity of 1-D ferrimagnets, with many choices in the size and nature (isotropic or anisotropic) of both magnetic moments and exchange interactions.[4-8]

The structure of this series (Figure 1) consists of infinite zigzag chains built up from two alternating octahedral sites bridged by carboxylate groups.[9,10] Further, due to the presence of two different bridging carboxylate topologies, the magnetic centers are also alternating, and so there is alternation not only of the magnetic sites but also of the exchange interactions. Then, the alternating chain may be schematized as

...-$M(H_2O)_4O_2$---M'(EDTA)-$M(H_2O)_4O_2$---M'(EDTA)-...

where dashed and full lines refer to the two different exchange pathways, J and J'; [$M(H_2O)_4O_2$] and [M'(EDTA)] correspond to the hydrated and chelated sites, respectively.

From the analysis of specific heat and susceptibility measurements, significant differences in the degree of exchange alternation have been emphasized, depending on the nature of the interacting ions.[4-7] Thus, while [MnNi] behaves as a uniform chain ($J'/J = 1$), members containing high-spin cobalt(II), as for example [CoCo] and [CoCu], show a drastic alternation, behaving as "quasi"-isolated dimers ($J'/J < 0.01$). This surprising result is difficult to attribute to a structural effect, since intermetallic distances and bridging angles remain almost constant in all the members of the series, so that an orbital effect needs to be invoked. In fact, we suggested that the large alternation of the cobalt-containing chains is likely to be related to the strong anisotropy of this ion. Due to the zigzag structure of chains, the **g** tensor of cobalt on each site would present different orientations with respect to the principal magnetic axes, and two different exchange components are expected, even in the absence of structural alternation.[5,6]

In order to discuss this possibility, the **g** tensors of cobalt on both sublattices are determined from a single-crystal EPR study on a Co-doped [ZnZn] sample. On the other hand, an EPR study of the ordered bimetallic chain [CoCu] is reported. In this system,

[†] Universidad de Valencia.
[‡] Universitâ di Firenze.

(1) Landee, C. P. In *Organic and Inorganic Low Dimensional Crystalline Materials*; Delhaes, P., Drillon, M., Eds.; NATO ASI Series B168; Plenum Press: New York, 1987.
(2) Kahn, O. *Struct. Bonding (Berlin)* **1987**, *68*, 89.
(3) Caneschi, A.; Gatteschi, D.; Sessoli, R.; Rey, P. *Acc. Chem. Res.* **1989**, *22*, 392.
(4) Coronado, E. In *Magnetic Molecular Materials*; Gatteschi, D., Kahn, O., Miller, J. L., Palacio, F., Eds.; NATO ASI Series E198. Kluwer Academic Publishers: Dordrecht, The Netherlands, 1991.
(5) Coronado, E.; Drillon, M.; Nugteren, P. R.; de Jongh, L. J.; Beltrân, D. *J. Am. Chem. Soc.* **1988**, *110*, 3907.
(6) Coronado, E.; Drillon, M.; Nugteren, P. R.; de Jongh, L. J.; Beltrân, D.; Georges, R. *J. Am. Chem. Soc.* **1989**, *111*, 3874.
(7) Coronado, E.; Sapiña, F.; Drillon, M.; de Jongh, L. J. *J. Appl. Phys.* **1990**, *67*, 6001.
(8) Drillon, M.; Coronado, E.; Gianduzzo, J. C.; Curely, J.; Georges, R. *Phys. Rev.* **1989**, *B40*, 10992.
(9) Coronado, E.; Drillon, M.; Fuertes, A.; Beltrân, D.; Mosset, A.; Galy, J. *J. Am. Chem. Soc.* **1986**, *108*, 900.
(10) McCandlish, E. F. K.; Michael, T. K.; Neal, J. A.; Lingafelter, E. C.; Rose, N. J. *Inorg. Chem.* **1978**, *17*, 1383.

0020-1669/92/1331-0294$03.00/0